Article

The Influence of Chitosan on Water Absorption and Solubility of Calcium Phosphate Cement

Ioana Lacan [1], Mărioara Moldovan [2] and Ioan Ardelean [1,*]

1   Department of Physics and Chemistry, Technical University of Cluj-Napoca, 400114 Cluj-Napoca, Romania; ioana_lacan@yahoo.com
2   "Raluca Ripan" Chemistry Research Institute, Department of Polymer Composites, "Babes-Bolyai" University, 400294 Cluj-Napoca, Romania; marioara.moldovan@ubbcluj.ro
*   Correspondence: ioan.ardelean@phys.utcluj.ro

Abstract: Calcium phosphate cements are widely used biomaterials for bone regeneration due to their biological properties, such as biocompatibility, biodegradability, and bioactivity. The presence of chitosan in cement composition influences the resorption rate of the material and its mechanical properties. In the present work, the water absorption and solubility of a tricalcium phosphate bone cement, prepared with and without chitosan addition, was comparatively evaluated. The absorption and solubility properties were monitored for 21 days by immersing the samples in water at room temperature and then weighing them. A morphological analysis of the samples was carried out via scanning electron microscopy (SEM). The absorption dynamics and pore evolution were investigated with low-field nuclear magnetic resonance (NMR) relaxometry. It was demonstrated that the presence of chitosan accelerates the hardening dynamics, reduces water absorption, and influences the solubility and degradation behavior of the cement. It was also observed that, independent of the presence of chitosan, the polymerization process is not completed even after one hour, which influences the solubility process. It was also shown that the presence of chitosan reduces the amount of microcracks and improves the functional properties of the hardened cement.

Keywords: absorption; bone cements; calcium phosphate; chitosan; NMR relaxometry

1. Introduction

Over the past 50 years, research has focused on the development of medical materials for skeletal repair and reconstructive surgery. Bioceramics, a highly attractive material for implants due to its composition being similar to that of bone tissue, has gained significant attention due to its importance in various medical applications [1]. Calcium phosphate (CaP)-based materials are widely used due to their excellent chemical properties and good biocompatibility with hard tissues [2]. That is why such synthetic materials are used in the medical field to repair bone defects [3].

Calcium phosphate cements (CPCs) have revolutionized the medical field of bone grafting, offering biocompatibility, osteoconductivity, resorbability, mouldability, and injectability [3]. CPCs are biomaterials that are extensively employed in clinical applications for repairing and reconstructing bone defects due to their ability to promote bone regeneration [4]. Depending on the final product, CPCs are divided into two categories: apatite and brushite cements [5]. Apatite cements are similar to the mineral phase of natural bone and can form precipitated hydroxyapatite (PHA) or calcium-deficient hydroxyapatite (CDHA) through a precipitation reaction. Brushite CPCs are obtained from an acid-base reaction; the most well-known and used basic reagent is tricalcium phosphate because it is more soluble than hydroxyapatite [6,7]. Brushite cements, obtained by Mirtchi et al. [8], have faster setting times and higher resorbability under physiological conditions. They are degraded by simple chemical dissolution, while apatite requires osteoclast activity. Brushite cements

are particularly useful for applications requiring bone replacement, while apatite cements have better mechanical strength [9,10].

Tricalcium phosphate (TCP) is a material used as a tissue substitute for the repair of bone defects because it is bioresorbable and biocompatible, as well as having interconnected microporosity. It is found in two allotropic forms, which are obtained at high temperatures and stabilize at room temperature [11]: α-TCP is soluble in aqueous solutions and easily transforms into calcium-deficient hydroxyapatite, and β-TCP is one of the most commonly used bone graft replacement materials because its solubility is similar to that of the mineral component of bone [12]. With all these beneficial characteristics, TCP-based biomaterials also have disadvantages related to limited biocompatibility and increased fragility. To improve certain biological and mechanical properties, various natural additives such as collagen, gelatin, or chitosan can be incorporated inside TCP-based cements [13,14].

Chitosan (CS) is a natural polymer utilized in a variety of applications due to its excellent properties [15]. It has been widely studied in tissue engineering for two decades. CS is soluble in an acidic environment and not at a neutral pH; it has a hydrophilic character, meaning that it absorbs water when immersed in it. Moreover, due to its intramolecular hydrogen bonding, it has a strong resistance to heat [16]. Incorporating chitosan into calcium phosphate cements provides advantages such as enhanced bioactivity, antibacterial properties, improved mechanical properties, drug delivery capabilities, and biocompatibility, making it a promising addition to CPC formulations for bone defect repair [17–20].

The water absorption capacity of a calcium phosphate cement is important for its clinical applications [21]. The pore structure and degree of hydration of a cement depends on the polymerization system and temperature [22]. The introduction of water into the polymer network has harmful as well as beneficial effects on the properties of the material [21,23]. Exposure to water can reduce the lifetime of cements through the hydrolysis of the bonding agent or filler, leading to microcracks and thus to a decrease in mechanical properties [24,25]. Therefore, the investigation of the water absorption behavior of bone cements is an important issue.

Most investigations regarding the water absorption behavior of bone cements are performed by immersing and analytically weighing the polymerized cement samples, according to the manufacturer, during a certain time interval, either immediately following the polymerization process or at a maximum of 21 days. Water capture follows the laws of diffusion, and the introduction of a more hydrophilic monomer gives rise to an increase in the absorption rate and diffusion coefficient, which can be significantly affected by changes in the powder/liquid ratio [26].

The dynamics of absorption and solubility can also be studied using low-field NMR relaxometry techniques. Such techniques were already used not only to study the structural properties and composition of human bone [27], but also to characterize the porosity and pore size distribution in compact bone [28]. Note, however, that knowledge of the relaxivity constant is necessary if obtaining the absolute pore sizes is envisaged. The main advantages of NMR relaxometry investigations over other techniques are that the samples do not require prior preparation, and information can be extracted not only about the dynamics of water molecules but also about the evolution of porous structures [29,30].

In the present work, comparative investigations regarding the absorption and solubility behavior of two CPCs, prepared with and without chitosan, are considered. The samples are immersed in water under the same conditions. The water content is determined both by weighing the samples and via NMR relaxation measurements at certain time intervals. On this basis, information about water absorption and sample solubility will be extracted. The surface of the sample is analyzed using scaning electron microscopy (SEM) to observe the eventual cracks.

2. Materials and Methods

2.1. Sample Preparation

Two samples made of calcium phosphate cements, denoted C1 and C2, respectively, were investigated, with the composition comprehensively discussed in our previous work [30]. The samples have the same solid–liquid ratios and identical quantity of liquid components and chemical initiation system. The C1 sample was prepared only using TCP, while the C2 sample was prepared by partially replacing the TCP with chitosan. The chitosan used in the preparation owns a high degree of deacetylation (>85%), and a molecular weight of 190–375 kDa, as determined by the manufacturer (Sigma-Aldrich Co., Schnelldorf, Germany). It is known that this aspect positively influences the sample's mechanical properties and solubility [31,32].

The liquid phase of the cement mixture is composed of urethane dimethacrylate (UDMA, 3%), an organic monomer with a large and rigid structure; hydroxyethyl methacrylate (HEMA, 25%), which acts as a viscosity modifier; and polyethylene glycol (PEG 400, 22%), an ingredient that has low-level toxicity and is very hydrophilic [33]. The organic matrix influences the properties of the cement, such as the amount of unreacted monomer, fluid absorption, and mechanical properties. The solid phase is composed of bioactive and biodegradable tricalcium phosphate (TCP, 50% from sample mass) for the C1 sample. In the case of the C2 sample, tricalcium phosphate is partially substituted by chitosan (25% TCP and 25% CS), which favors better osteo-integration [13].

For the process of hardening the sample, a chemical polymerization system was used, which assumes that the paste obtained by mixing the two phases should be divided into two equal proportions: one in which the polymerization initiator benzoyl peroxide (BPO) is added in proportion to 2% of the paste mass and the other in which dihydroxy ethyl-p-toluidine (DHEPT) polymerization accelerator is dissolved in a proportion of 0.75% of the paste. By mixing the equal proportions of the two pastes, the polymerization takes place, which leads to the formation of the hardened material. The hardened materials are presented as homogeneous solids with a smooth and glossy surface consisting of a single phase, in which the inorganic filler is chemically linked to the polymer matrix.

2.2. Absorption and Solubility Tests

Absorption and solubility tests were conducted following the ISO 4049 practice [34,35]. However, in this study, the test samples were prepared using a cylindrical glass mold with a 4 mm diameter and 5 mm thickness to fit inside an NMR tube. The shape was filled in with cement and covered with glass to obtain a smooth and homogeneous surface of the hardened material. After the polymerization time expired (3.5 min after mixing the 2 pastes), the samples were extracted from the mold and were conditioned in a desiccator at 22 °C until a constant mass was obtained (initial mass, m_0). After this stage, the C1 and C2 cement samples were immersed, individually, in containers with distilled water at room temperature (about 22 °C) for 21 days. At different time intervals of 1, 3, 7, 14, and 21 days, respectively, the samples were removed from the immersion medium and gently dried with absorbent paper. Each sample was then immediately weighed using an analytical balance with a precision of 0.001 g, obtaining the m_1 mass of the saturated sample. The weighed samples were then stored for four hours in a desiccator until a constant mass, m_2, was obtained. The water absorption (*WA*) and solubility (*WS*) of the materials were calculated as percentages from the initial mass, m_0, according to the formulas [25,32]:

$$WA(\%) = \frac{m_1 - m_0}{m_0} \times 100;$$ (1)

and

$$WS(\%) = \frac{m_0 - m_2}{m_0} \times 100.$$ (2)

In addition to the absorption and solubility tests, we also monitored the normalized sample mass after it was extracted from the desiccator which shows the evolution of the sample degradability.

2.3. NMR Relaxometry Experiments

Transverse relaxation measurements were performed at 35 Celsius using a low-field NMR instrument operating at 20 MHz proton resonance frequency (Minispec MQ20, Bruker, Heidelberg, Germany) and the well-known Carr–Purcell–Meiboom–Gill (CPMG) radiofrequency pulse sequence [30]. The CPMG pulse sequence generates a train of spin echoes separated by an echo time interval. The amplitudes of these echoes are attenuated by the transverse relaxation phenomena, which allows the effective transverse relaxation time distributions to be extracted. This technique is fast and thus enables multiple accumulations of the echo train signals, resulting in an enhanced signal-to-noise ratio.

In the case of a heterogeneous sample, the presence of a distribution of transverse relaxation times determines the CPMG echo train to exhibit multiple-exponential decay. To extract the relaxation time distribution, a numerical Laplace inversion algorithm can be applied to the CPMG echo train [36,37]. Note, however, that numerical Laplace inversion is ill-conditioned and the extracted relaxation time distributions may be affected by noise; consequently, comparative tests on theoretically generated echo trains were carried out before analyzing the experimental data. In the present work, the echo train recorded was composed of 1000 echoes with an echo time interval of 100 μs. Note that, the combination between a low-field NMR instrument and the short echo time intervals provides the conditions necessary to neglect diffusion effects on echo train attenuation [29].

2.4. Microstructural Analysis of Cements

The surface of cement samples was investigated via scanning electron microscopy techniques (SEM-Inspect S, FEI, Eindhoven, The Netherlands). The electron microscopy image was recorded at 15 KV with a magnification of 1000×. The surface of the two samples was analyzed before introducing them into distilled water and after 21 days of immersion.

3. Results and Discussion

Water absorption can influence both the microstructure and the mechanical properties of calcium phosphate cements. That is why, in the present work, the absorption behavior of CPCs with and without chitosan was investigated during the 21-day interval. To understand the absorption process, the hardening dynamics of the two samples were investigated first, via NMR relaxometry. Thus, we recorded the CPMG echo trains of the dry samples, that is, without immersing them into water. The echo trains depicted in Figure 1 indicate a slower hardening process in the case of the C1 sample (Figure 1a) as compared with C2 sample (Figure 1b), which contains chitosan. This observation for longer hardening times is analogous with the previous results on similar samples for shorter evolution times [30]. It is also observed that for both samples, the polymerization process is not completely finalized even after one hour, and this may affect both the absorption and solubility dynamics. However, the hardening process for both samples is complete after 24 h, when no changes in the relaxation time distributions were detected anymore, as demonstrated in Figure 1.
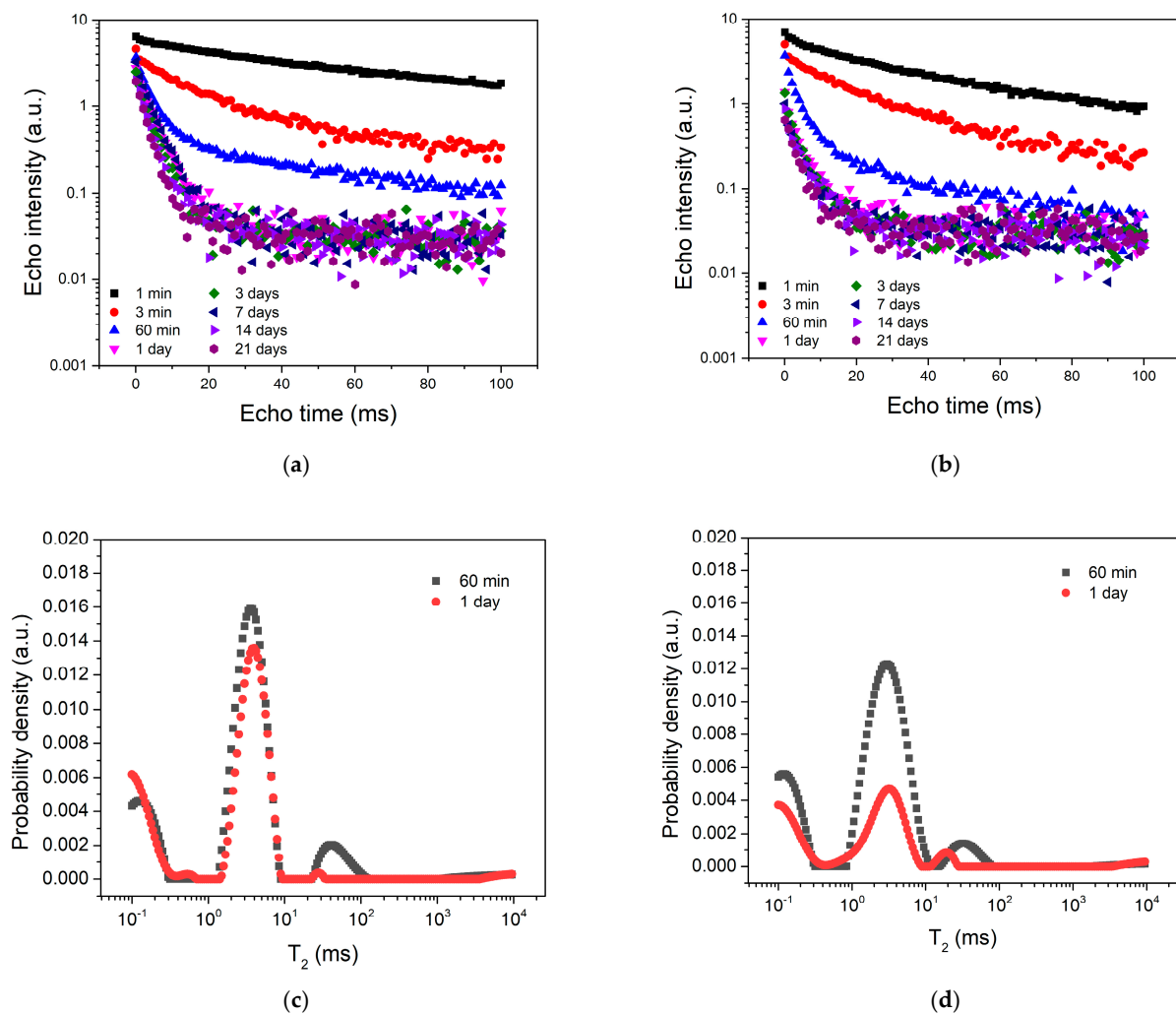
(a)

(b)

(c)

(d)

Figure 1. CPMG echo trains recorded at different hardening times from the end of the mixing process for both samples, C1 (**a**) and C2 (**b**), respectively. The comparison of the relaxation time distributions extracted at 1 h and 1 day of hardening for the C1 sample (**c**) and the C2 sample (**d**), respectively.

The relaxation time distributions displayed in Figure 1c,d indicate a consumption of the mobile component, characterized by relaxation times between 1 ms and 10 ms, within the first day, for both samples. This mobile component is transformed into a quasi-solid component with relaxation times shorter than 0.3 ms, only partially detectable with low-field NMR relaxometry [30]. One can also observe a longer relaxation time component (10–100 ms) even after 1 day of hardening, which could be associated with the residual monomers. Comparing the two samples, we notice a stronger consumption of the mobile component during the hardening interval for the sample containing chitosan (C2) as compared with the sample only containing TCP.

The results of absorption tests for the two composites during the 21 days of absorption are indicated in Figure 2a. One can observe that the cement sample without chitosan (C1) shows an increased absorption until day 7, when the maximum value is reached, followed by a gradual decrease until day 21. This increase in water absorption can be influenced by hydrophilic components with phosphate groups or carboxylic groups [16]. Huang et al. [38] observed that water absorption leads, over time, to matrix swelling, hydrolytic degradation, and decreased mechanical properties. For the sample containing chitosan (C2), the maximum water absorption was recorded on the first day, followed by a gradual decrease until day 21. Due to its hydrophilic character, chitosan absorbs water

at room temperature [39]. Furthermore, during the whole investigation period, water absorption was reduced by the partial replacement of TCP with chitosan in the C2 sample.
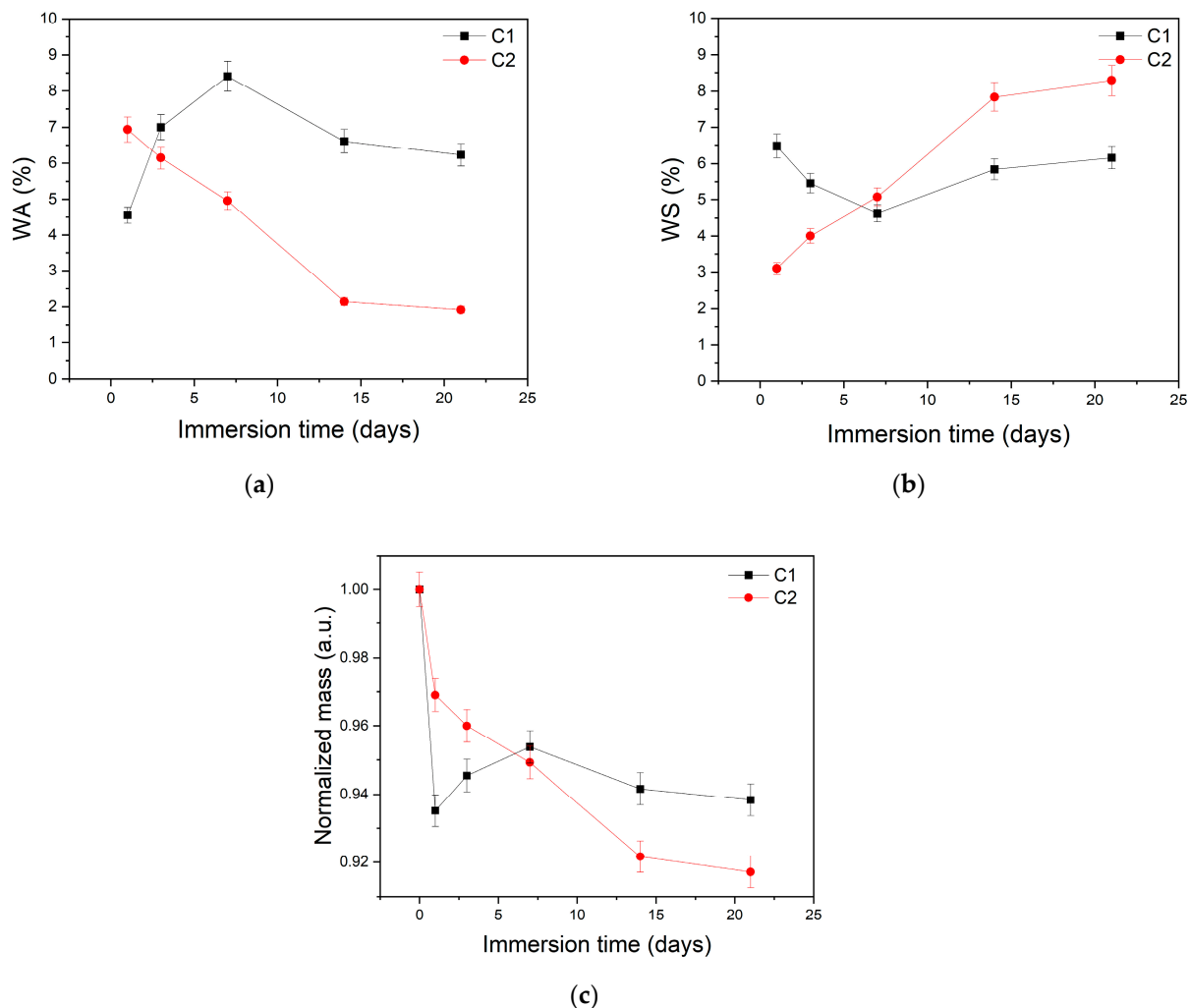

(a)

(b)

(c)

Figure 2. Evolution of water absorption (**a**), water solubility (**b**) and the normalized sample mass (**c**) during the 21-day interval for the two bone cements, as indicated in the legend.

As a result of water diffusion, the solubility of the polymer matrix increases. Thus, the values obtained for the C1 sample (Figure 2b) show a gradual decrease until day 7, when the lowest solubility value, calculated on the basis of Equation (2), was recorded. Then, a gradual increase until day 21 follows, but the solubility value does not exceed its value on the first day. This behavior can be explained by the solubilization of TCP during the first days and represents the reason why TCP is often used as a drug carrier due to its ion exchange capacity [40]. For the C2 sample, over the entire reference interval, even from the first day, there is a gradual increase in solubility, this evolution being influenced by the high degree of deacetylation of chitosan (>85%) [14,41].

The degradation of the two samples is also revealed by their normalized mass evolution shown in Figure 2c. One can observe that the C1 sample experiences an important mass loss of approximately 7% on the first day, followed by an increase in mass until day 7. This increase may be influenced by the amount of liquid absorbed by the cement until day 7, when the sample is supersaturated. Then follows a mass decrease in the forthcoming time intervals, but the mass reached on day 21 is not lower than the mass on the first day. This evolution can be affected by the polymerization process, which is not finalized when the sample is introduced into the liquid, but can also be influenced by the TCP degradability [13], a process that affects the microstructure and mechanical

properties of the cement [42]. The C2 sample revealed the steepest mass loss during the first day, followed by a gradual decrease until day 21, when a total loss of approximately 7% was recorded. The degradation behavior of chitosan may influence this result [9,42]. The degradation of chitosan in distilled water takes place through the residual OH and NH_2 groups that interact with water molecules through hydrogen bonds [43].

The SEM images of the investigated materials before immersion (Figure 3a,b) reveal the presence of air inclusions (indicated by arrows) incorporated after the process of polymerization and sample manipulation. After 21 days of immersion, both samples show surface defects, resulting from the absorption and solubility process. Most of the microcracks are observed in the TCP sample (Figure 3c).
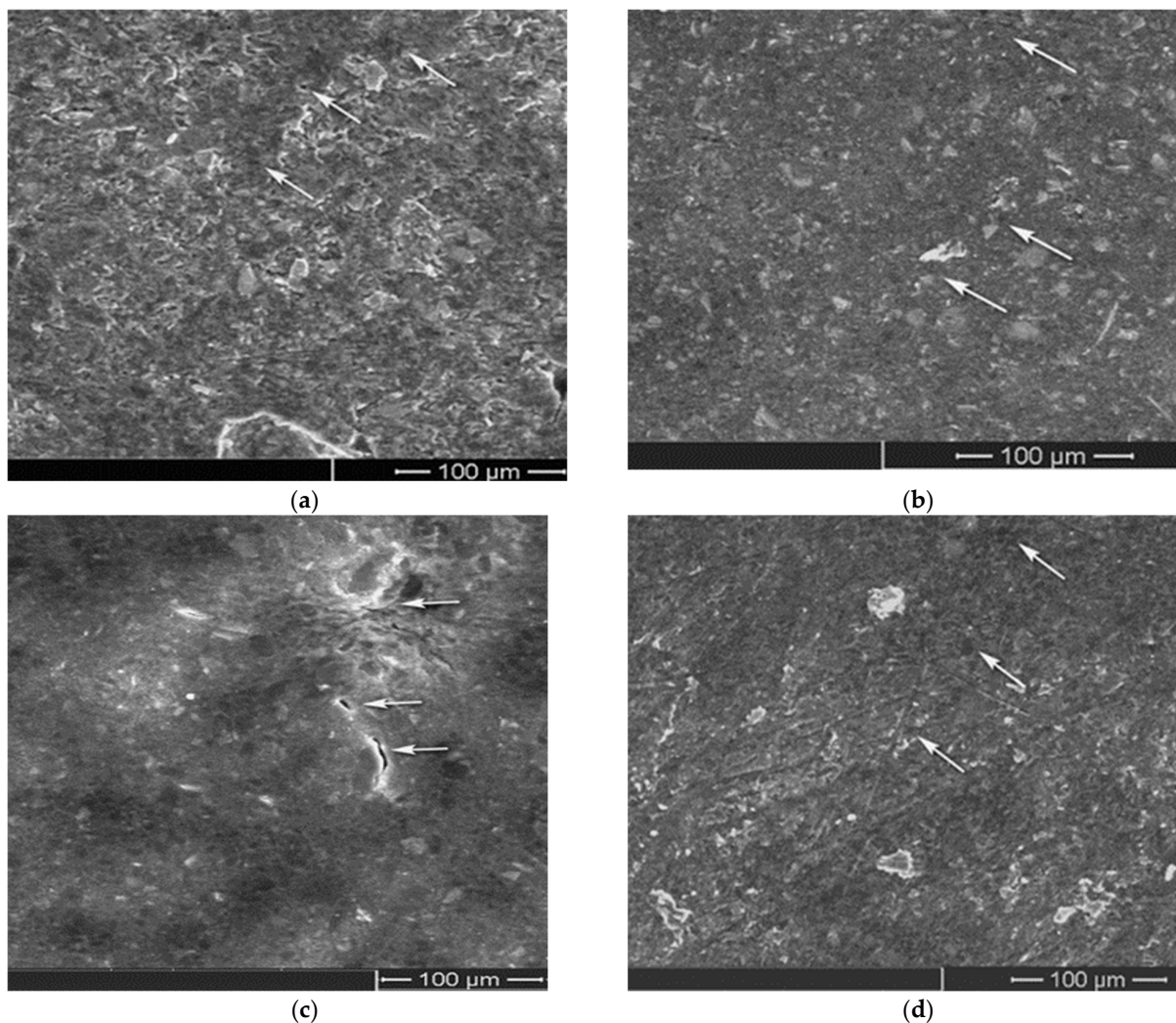

Figure 3. SEM images the two cements: (**a**) sample C1 before being introduced into the liquid; (**b**) sample C2 before being introduced into the liquid; (**c**) sample C1 after 21 days of immersion in distilled water; (**d**) sample C2 after 21 days of immersion in distilled water.

The porosity of CPCs is a significant factor because it influences the degradation rate and mechanical properties of the sample. Information about porosity and water absorption of bone cements can be obtained via low-field nuclear magnetic resonance relaxometry. Figure 4 shows the relaxation time distributions before (empty sample at 1 h hardening time) and after water absorption (1, 3, 7, 14, 21 days) for the C1 sample (Figure 4a), containing only TCP, and the C2 sample (Figure 4b), also containing chitosan. Analyzing the relaxation time distributions, a series of peaks can be observed, with an additional half peak, visible for both samples, that appears during the interval between 0.1 and 0.3 ms and which may

correspond to the quasi-solid component of the cement composites [5,7,44]. The other peaks, arising after 0.3 ms, can be attributed to the more mobile components, such as mobile polymer networks or liquid components inside sample pores (HEMA and PEG), not participating in the reaction (unreacted monomers) [30].
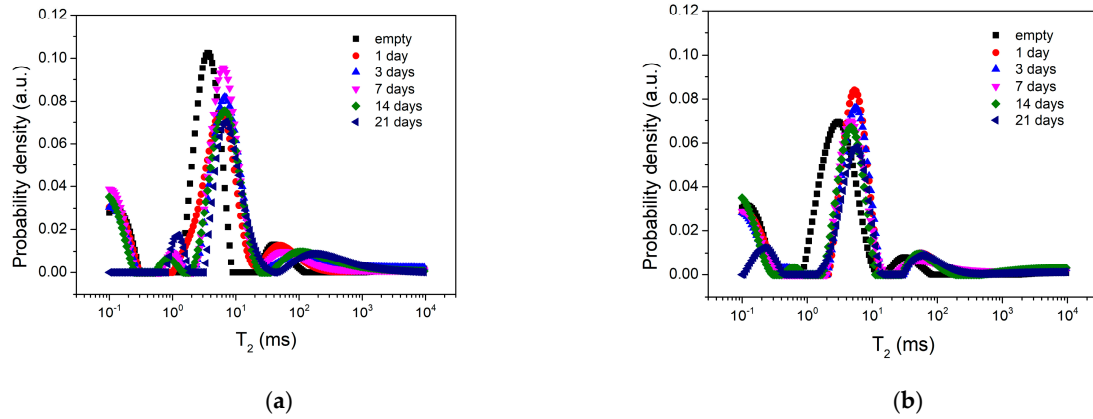

(a)

(b)

Figure 4. Relaxation time distributions obtained with a numerical Laplace transformation of the CPMG echo trains recorded during the water absorption of the two cement samples, C1 (**a**) and C2 (**b**), respectively.

As can be observed from Figure 4, the largest peak, between 2 ms and 30 ms, which can be associated with a component with a higher degree of mobility [30] than the quasi-solid component (0.1–0.3 ms), shifts to larger values of relaxation time during absorption. Note that this evolution is not present in the case of dry samples during hardening (see Figure 1c,d); consequently, it must be caused by water absorption. Figure 5a also shows longer values of the relaxation time in the case of the C1 sample as compared to the C2 sample. These values could be associated with the presence of smaller pores inside the C2 sample, containing chitosan, which explains the lower absorption coefficients, WA, in Figure 2a. The third peak, arising in the interval of 30–1000 ms, may be associated with the residual monomers, but this peak could also represent water-filled voids. These voids may be caused by the air in the polymer powder (see Figure 3a,b) and be remanent inside the sample during the mixing process. Over time, these voids can reduce the strength of the hardened cement and can affect the function and the bone regeneration process [44,45].
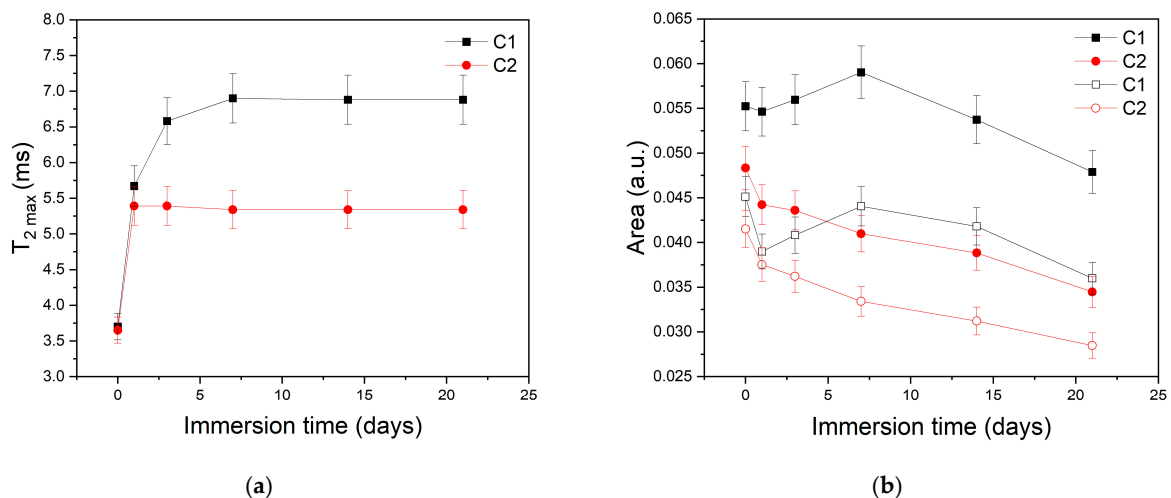

(a)

(b)

Figure 5. (**a**) The evolution of the largest peak maximum during the immersion time. (**b**) Evolution of the area associated with the mobile components, characterized by a relaxation time $T_2 > 2$ ms (filled symbols), and the area corresponding to the largest peak alone (empty symbols).

The area of the mobile components in the relaxation time distribution, characterized by relaxation times, T_2, longer than 2 ms, was also analyzed during absorption and the data are represented in Figure 5b (filled symbols). This area quantifies both the remaining mobile components after the polymerization process and the absorbed water, as they cannot be separated. Analyzing the areas, we notice smaller values in the case of the sample containing chitosan (C2) as compared with the sample only containing TCP (C1) for all absorption intervals. As can be observed, the area increases in the case of the C1 sample until day 7, followed by a decrease on days 14 and 21. For the C2 sample, supersaturation is recorded on the very first day, after which the absorption decreases with the advance in time. These observations are in agreement with the previous studies, which concluded that supersaturation can be influenced by the concentration of calcium and phosphate ions in the solution. These minerals are necessary to support bone mineralization and are very important for human physiology [30,45]. Furthermore, the NMR results are, to a certain degree, similar to the absorption results shown in Figure 1a. Comparing the areas of the largest peak (empty symbols in Figure 5b) with the total area of the mobile component (characterized by $T_2 > 2$ ms) we can observe a significant difference in the case of the C1 sample and a somewhat smaller one for the C2 sample, containing chitosan. These differences in the area may indicate the presence of microcracks within the samples, particularly observed in the case of the C1 sample (Figure 3c). In time, these microcracks have the potential to contribute to the failure of the cement [46].

4. Conclusions

The water absorption and solubility tests conducted on two tricalcium phosphate cements, prepared with and without the partial replacement of tricalcium phosphate with chitosan, have demonstrated that the inclusion of chitosan leads to a reduction in water absorption and solubility. Both samples undergo mass loss during water immersion but follow distinct patterns. The solubility of the polymer matrix decreases until day 7 for the sample without chitosan, while it gradually increases for the sample containing chitosan. Furthermore, by the partial replacement of tricalcium phosphate with chitosan a faster hardening process takes place. However, the polymerization is not fully completed even after one hour, and both samples reach complete hardening only after 24 h. Low-field nuclear magnetic resonance relaxometry experiments have revealed smaller pores in the sample containing chitosan and less microcracks. In summary, the addition of chitosan accelerates hardening dynamics, reduces water absorption, and affects solubility and degradation behavior. The studies performed here under in vitro conditions highlight the potential of chitosan as a modifier to enhance the properties of cement samples, and it would be worth considering them also under in vivo conditions.

Author Contributions: Conceptualization, I.L., M.M. and I.A.; methodology, I.A. and M.M.; investigation, I.L. and I.A.; resources, M.M. and I.A.; writing—original draft preparation, I.L.; writing—review and editing, I.A., I.L. and M.M.; supervision, I.A.; project administration, I.A.; funding acquisition, I.A. All authors have read and agreed to the published version of the manuscript.

Institutional Review Board Statement: Not applicable.

Informed Consent Statement: Not applicable.

Data Availability Statement: Data may be provided on request from the corresponding author.

References

1. Goh, K.W.; Wong, Y.H.; Ramesh, S.; Chandran, H.; Krishnasamy, S.; Sidhu, A.; Teng, W. Effect of pH on the properties of eggshell-derived hydroxyapatite bioceramic synthesized by wet chemical method assisted by microwave irradiation. *Ceram. Int.* **2021**, *47*, 8879–8887. [CrossRef]
2. Hou, X.; Zhang, L.; Zhou, Z.; Luo, X.; Wang, T.; Zhao, X.; Lu, B.; Chen, F.; Zheng, L. Calcium Phosphate-Based Biomaterials for Bone Repair. *J. Funct. Biomater.* **2022**, *13*, 187. [CrossRef]
3. Wong, S.K.; Wong, Y.H.; Chin, K.-Y.; Ima-Nirwana, S. A Review on the Enhancement of Calcium Phosphate Cement with Biological Materials in Bone Defect Healing. *Polymers* **2021**, *13*, 3075. [CrossRef]
4. Koons, G.L.; Diba, M.; Mikos, A.G. Materials design for bone-tissue engineering. *Nat. Rev. Mater.* **2020**, *5*, 584–603. [CrossRef]
5. Ginebra, M.-P.; Montufar, E.B. *Cements as Bone Repair Materials*; Woodhead Publishing Series in Biomaterials: Cambridge, UK, 2019; pp. 233–271. [CrossRef]
6. Destainville, A.; Champion, E.; Bernache-Assollant, D.; Laborde, E. Synthesis, characterization and thermal behavior of apatitic tricalcium phosphate. *Mater. Chem. Phys.* **2003**, *80*, 269–277. [CrossRef]
7. Lodoso-Torrecilla, I.; Beucken, J.v.D.; Jansen, J. Calcium phosphate cements: Optimization toward biodegradability. *Acta Biomater.* **2020**, *119*, 1–12. [CrossRef]
8. Mirtchi, A.A.; Lemaitre, J.; Terao, N. Calcium phosphate cements: Study of the β-tricalcium phosphate—Monocalcium phosphate system. *Biomaterials* **1989**, *10*, 475–480. [CrossRef]
9. Hurle, K.; Christel, T.; Gbureck, U.; Moseke, C.; Neubauer, J.; Goetz-Neunhoeffer, F. Reaction kinetics of dual setting α-tricalcium phosphate cements. *J. Mater. Sci. Mater. Med.* **2016**, *27*, 1–13. [CrossRef]
10. Hurle, K.; Oliveira, J.; Reis, R.; Pina, S.; Goetz-Neunhoeffer, F. Ion-doped Brushite Cements for Bone Regeneration. *Acta Biomater.* **2021**, *123*, 51–71. [CrossRef]
11. Rey, C.; Combes, C.; Drouet, C.; Grossin, D.; Bertrand, G.; Soulié, J. 1.11 Bioactive Calcium Phosphate Compounds: Physical Chemistry. *Compr. Biomater. II* **2017**, *1*, 187–221. [CrossRef]
12. Bohner, M.; Santoni, B.L.G.; Döbelin, N. β-tricalcium phosphate for bone substitution: Synthesis and properties. *Acta Biomater.* **2020**, *113*, 23–41. [CrossRef]
13. Fang, C.-H.; Lin, Y.-W.; Sun, J.-S.; Lin, F.-H. The chitosan/tri-calcium phosphate bio-composite bone cement promotes better osteo-integration: An in vitro and in vivo study. *J. Orthop. Surg. Res.* **2019**, *14*, 162. [CrossRef]
14. Ikeda, T.; Ikeda, K.; Yamamoto, K.; Ishizaki, H.; Yoshizawa, Y.; Yanagiguchi, K.; Yamada, S.; Hayashi, Y. Fabrication and Characteristics of Chitosan Sponge as a Tissue Engineering Scaffold. *BioMed Res. Int.* **2014**, *2014*, 1–8. [CrossRef] [PubMed]
15. Rinaudo, M. Chitin and chitosan: Properties and applications. *Prog. Polym. Sci.* **2006**, *31*, 603–632. [CrossRef]
16. Piekarska, K.; Sikora, M.; Owczarek, M.; Jóźwik-Pruska, J.; Wiśniewska-Wrona, M. Chitin and Chitosan as Polymers of the Future—Obtaining, Modification, Life Cycle Assessment and Main Directions of Application. *Polymers* **2023**, *15*, 793. [CrossRef] [PubMed]
17. Shi, Z.; Neoh, K.; Kang, E.; Wang, W. Antibacterial and mechanical properties of bone cement impregnated with chitosan nanoparticles. *Biomaterials* **2006**, *27*, 2440–2449. [CrossRef] [PubMed]
18. Kim, Y.; Zharkinbekov, Z.; Raziyeva, K.; Tabyldiyeva, L.; Berikova, K.; Zhumagul, D.; Temirkhanova, K.; Saparov, A. Chitosan-Based Biomaterials for Tissue Regeneration. *Pharmaceutics* **2023**, *15*, 807. [CrossRef] [PubMed]
19. Aguilar, A.; Zein, N.; Harmouch, E.; Hafdi, B.; Bornert, F.; Offner, D.; Clauss, F.; Fioretti, F.; Huck, O.; Jessel, B.; et al. Application of Chitosan in Bone and Dental Engineering. *Molecules* **2019**, *24*, 3009. [CrossRef]
20. Aranaz, I.; Alcántara, A.R.; Civera, M.C.; Arias, C.; Elorza, B.; Caballero, A.H.; Acosta, N. Chitosan: An Overview of Its Properties and Applications. *Polymers* **2021**, *13*, 3256. [CrossRef]
21. Sun, L.; Xu, H.H.K.; Takagi, S.; Chow, L.C. Fast setting calcium phosphate cement-chitosan composite: Mechanical properties and dissolution rates. *J. Biomater. Appl.* **2007**, *21*, 299–315. [CrossRef]
22. Pelletier, M.H.; Lau, A.C.B.; Smitham, P.J.; Nielsen, G.; Walsh, W.R. Pore distribution and material properties of bone cement cured at cifferent temperatures. *Acta Biomater.* **2010**, *6*, 886–891. [CrossRef]
23. Roy, J.C.; Salaün, F.; Giraud, S.; Ferri, A. *Solubility of Chitin: Solvents, Solution Behaviors and Their Related Mechanisms Solubility of Chitin: Solvents, Solution Behaviors and Their Related Mechanisms*; IntechOpen: Rijeka, Croatia, 2017; pp. 109–127. [CrossRef]
24. Lim, J. *Stress Corrosion Cracking (SCC) in Polymer Composites*; Woodhead Publishing: Cambridge, UK, 2011; pp. 485–536. [CrossRef]
25. Slane, J.; Vivanco, J.; Meyer, J.; Ploeg, H.-L.; Squire, M. Modification of acrylic bone cement with mesoporous silica nanoparticles: Effects on mechanical, fatigue and absorption properties. *J. Mech. Behav. Biomed. Mater.* **2014**, *29*, 451–461. [CrossRef] [PubMed]
26. Pascual, B.; Gurruchaga, M.; Ginebra, M.; Gil, F.; Planell, J.; Goñi, I. Influence of the modification of P/L ratio on a new formulation of acrylic bone cement. *Biomaterials* **1999**, *20*, 465–474. [CrossRef] [PubMed]

27. Barbieri, M.; Fantazzini, P.; Testa, C.; Bortolotti, V.; Baruffaldi, F.; Kogan, F.; Brizi, L. Characterization of Structural Bone Properties through Portable Single-Sided NMR Devices: State of the Art and Future Perspectives. *Int. J. Mol. Sci.* **2021**, *22*, 7318. [CrossRef] [PubMed]

28. Ni, Q.; King, J.D.; Wang, X. The characterization of human compact bone structure changes by low-field nuclear magnetic resonance. *Meas. Sci. Technol.* **2004**, *15*, 58–66. [CrossRef]

29. Pop, A.; Ardelean, I. Monitoring the size evolution of capillary pores in cement paste during the early hydration via diffusion in internal gradients. *Cem. Concr. Res.* **2015**, *77*, 76–81. [CrossRef]

30. Lacan, I.; Moldovan, M.; Sarosi, C.; Ardelean, I. Chitosan Effect on Hardening Dynamics of Calcium Phosphate Cement: Low-Field NMR Relaxometry Investigations. *Polymers* **2022**, *14*, 3042. [CrossRef]

31. Lv, S. High-performance superplasticizer based on chitosan. In *Biopolymers and Biotech Admixtures for Eco-Efficient Construction Materials*; Elsevier: Amsterdam, The Netherlands, 2016; pp. 131–150. [CrossRef]

32. Craciun, A.; Prodan, D.; Constantiniuc, M.; Ispas, A.; Filip, M.; Moldovan, M.; Badea, M.; Petean, I.; Crisan, M. Stability of Dental Composites in Water and Artificial Saliva. *Mater. Plast.* **2020**, *57*, 57–66. [CrossRef]

33. Handal, J.A.; Tiedeken, N.C.; Gershkovich, G.E.; Kushner, J.A.; Dratch, B.; Samuel, S.P. Polyethylene glycol improves elution properties of polymethyl methacrylate bone cements. *J. Surg. Res.* **2015**, *194*, 161–166. [CrossRef]

34. Müller, J.A.; Rohr, N.; Fischer, J. Evaluation of ISO 4049: Water sorption and water solubility of resin cements. *Eur. J. Oral Sci.* **2017**, *125*, 141–150. [CrossRef]

35. Labban, N.; AlSheikh, R.; Lund, M.; Matis, B.A.; Moore, B.K.; Cochran, M.A.; Platt, J.A. Evaluation of the Water Sorption and Solubility Behavior of Different Polymeric Luting Materials. *Polymers* **2021**, *13*, 2851. [CrossRef]

36. Venkataramanan, L.; Song, Y.Q.; Hurlimann, M.D. Solving Fredholm integrals of the first kind with tensor product structure in 2 and 2.5 dimensions. *IEEE Trans. Signal Process.* **2002**, *50*, 1017–1026. [CrossRef]

37. Huang, C.; Fu, S.; Zhang, Y.; Lauke, B.; Li, L.; Ye, L. Cryogenic properties of SiO_2/epoxy nanocomposites. *Cryogenics* **2006**, *45*, 450–454. [CrossRef]

38. Ali, M. Synthesis and Characterization of the Composite Material PVA/Chitosan/5% Sorbitol with Different Ratio of Chitosan. *Int. J. Mech. Mechatron. Eng.* **2017**, *17*, 15–28.

39. Espanol, M.; Perez, R.; Montufar, E.; Marichal, C.; Sacco, A.; Ginebra, M. Intrinsic porosity of calcium phosphate cements and its significance for drug delivery and tissue engineering applications. *Acta Biomater.* **2009**, *5*, 2752–2762. [CrossRef] [PubMed]

40. Kołodziejska, M.; Jankowska, K.; Klak, M.; Wszoła, M. Chitosan as an Underrated Polymer in Modern Tissue Engineering. *Nanomaterials* **2021**, *11*, 3019. [CrossRef] [PubMed]

41. Beruto, D.T.; Mezzasalma, S.A.; Capurro, M.; Botter, R.; Cirillo, P. Use of -tricalcium phosphate (TCP) as powders and as an aqueous dispersion to modify processing, microstructure, and mechanical properties of polymethylmethacrylate (PMMA) bone cements and to produce bone-substitute compounds. *J. Biomed. Mater. Res.* **1999**, *49*, 498–505. [CrossRef]

42. Jayasuriya, A.C.; Mauch, K.J. In vitro degradation behavior of chitosan based hybrid microparticles. *J. Biomed. Sci. Eng.* **2011**, *04*, 383–390. [CrossRef]

43. Devi, D.A.; Smitha, B.; Sridhar, S.; Aminabhavi, T. Pervaporation separation of isopropanol/water mixtures through crosslinked chitosan membranes. *J. Membr. Sci.* **2005**, *262*, 91–99. [CrossRef]

44. Zhang, J.; Liu, W.; Schnitzler, V.; Tancret, F.; Bouler, J.-M. Calcium phosphate cements for bone substitution: Chemistry, handling and mechanical properties. *Acta Biomater.* **2014**, *10*, 1035–1049. [CrossRef]

45. Beppu, M.M.; Torres, M.A.; Aimoli, C.G.; Goulart, G.A.S.; Santana, C.C. In vitro mineralization on chitosan using solutions with excess of calcium and phosphate ions. *J. Mater. Res.* **2005**, *20*, 3303–3311. [CrossRef]

46. O'Brien, F.J.; Taylor, D.; Lee, T.C. The effect of bone microstructure on the initiation and growth of microcracks. *J. Orthop. Res.* **2005**, *23*, 475–480. [CrossRef] [PubMed]